

Chemistry—A European Journal

Supporting Information

Deinterpenetration of IRMOF-9

Audrey B. Crom, Joseph L. Strozier, Caleb J. Tatebe, Cassidy A. Carey, Jeremy I. Feldblyum,*
and Douglas T. Genna*

Table of Contents

General Considerations.....	3
Sample Preparation for UV-Vis Spectroscopy.....	3
Powder X-ray Diffraction Parameters.....	3
Experimental Procedures.....	4
Synthesis of IRMOF-9 ¹	4
Deinterpenetration of IRMOF-9.....	5
Dying of MOFs with Reichardt's Dye in DMF.....	5
Dying of MOFs with Ferrocene.....	6
Gas Sorption Measurements.....	8
Modeling of Pore Diameters.....	10
Supplemental Figures.....	11
References.....	29

General Considerations

4,4-Biphenyldicarboxylic acid (Alfa Aesar), Reichardt's dye (Sigma), Rhodamine B (TCI), were purchased from commercial sources and used as received. Tetraethylammonium bromide (Sigma) and zinc nitrate hexahydrate (Fisher Scientific) were dried at room temperature under reduced pressure (~0.5 mm Hg) overnight prior to use. Chloroform-d and dimethylsulfoxide-d₆ were purchased from Sigma-Aldrich and Cambridge Isotope Laboratories, respectively, and used as received. IRMOF-9 was prepared using previously reported methods.¹ Solvent external to the framework was removed under reduced pressure (~0.5 mm Hg) at room temperature for 24 hr before further manipulation.

TGA data were collected on a TA Instruments TGA Q50 from 40° C to 600° C at a rate of 10° C per minute. NMR data were collected on a 400 MHz Bruker Avance NMR Spectrometer.

Sample Preparation for UV-Vis Spectroscopy

UV-visible spectrometry was performed by charging a quartz cuvette charged with a 0.0032 M solution of Et₄NBr in 1:1 DMF:DCM (b/v) with the addition of dried IRMOF-9 (2 mg). Readings were obtained every 2 min for 5 hr.

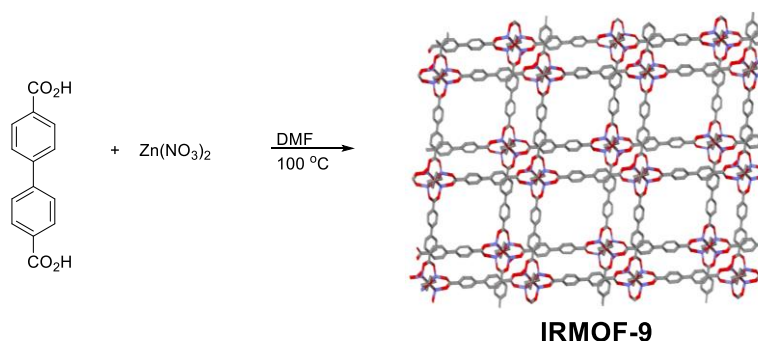
Powder X-ray Diffraction Parameters

Powder XRD patterns of small samples were collected on a Bruker AXS X8 Prospector CCD single crystal diffractometer using the "pilot" plugin for collection of multicrystalline XRD patterns. The instrument is equipped with a copper I μ S microsource with a laterally graded multilayer (Goebel) mirror for monochromatization ($\lambda = 1.54178$ Å, beam size 0.1-0.2 mm) and an ApexII CCD area detector. Powder samples were thoroughly ground to assure a representative number of crystallites to be present in the X-ray beam. Powder samples were mixed with small amounts of mineral oil and mounted onto a 0.4 mm diameter Mitegen micromesh mount for data collection. Samples were centered in the beam using the instrument's mounting microscope video camera. Data were collected in an emulated theta-2theta setup using the Apex2 software package of Bruker AXS. The sample mount was aligned horizontally ($\chi = 0^\circ$) and theta angles were set to eight different angles between 12 and 96° to cover a range equivalent to a 0 to 110° range of a powder X-ray diffractometer operated in Debye Scherrer mode (omega angles of each run were

set to half the theta values). Samples were rotated around the mount's spindle axis during measurement (360° rotation around ϕ), typical exposure times were 30 seconds per frame collected. The eight individual patterns taken were corrected for unequal sample to detector surface distance ("unwarped") and were combined into one continuous pattern using the "pilot plugin" software embedded in the Apex2 software package. Data were integrated over 2θ , converted in powder XRD patterns in Bruker .raw format and were further processed with standard powder XRD software packages.

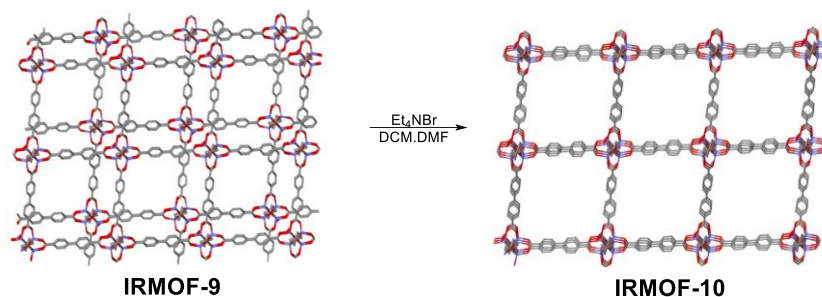
Experimental Procedures

Synthesis of IRMOF-9¹



To a 250 mL beaker charged with DMF (100 mL) was added $\text{Zn}(\text{NO}_3)_2$ hexahydrate (1.80 g, 6.1 mmol) and 4,4'-biphenyldicarboxylic acid (0.30 g, 1.2 mmol) and the resulting mixture was stirred for 15 minutes. The solution was filtered through a GE 25 mm PVDF syringe filter ($0.45\ \mu\text{m}$) in 6 mL portions, into 16 individual 20 mL scintillation vials. The vials were capped with Teflon-lined caps and then placed in an $100\ ^\circ\text{C}$ oven for 18 hr. At this time the vials were removed from the oven and allowed to cool to room temperature. The crystalline solids were then combined and washed with fresh DMF 3 x 10 mL. Crystalline MOF was suspended in fresh DMF until needed.

Deinterpenetration of IRMOF-9



To a 20 mL scintillation vial was added 30 mg of IRMOF-9, 3 mL of DMF, and a 0.32 M solution of TEABr (0.96 mmol) in DCM. The vial was then agitated on an orbital shaker at 75 rpm at room temperature for the appropriate time (note: complete reaction can be obtained in 2 days). The vial was removed from the shaker and the mother liquor was decanted. The remaining solids were washed with fresh DMF (3 x 3 mL), the liquid was decanted and the solids were characterized by PXRD, dye tests (described below), and TGA.

Dyeing of MOFs with Reichardt's Dye in DMF

As-synthesized IRMOF-9 (approximately 20 mg) or deinterpenetrated IRMOF-9 was submerged in 1 mL of a 10 mM solution of Reichardt's dye in DMF for a minimum 48 h. After 48 h, the crystals were removed from the dye solution, washed in fresh DMF, and examined using optical microscopy immediately after washing (both whole crystals and after cutting with a steel razor blade to obtain cross-sections). MOFs were examined under heavy mineral oil to prevent hydrolysis during analysis.

Dying of MOFs with Ferrocene

As-synthesized IRMOF-9 or deinterpenetrated IRMOF-9 (ca. 15 mg) was submerged in 1 mL of a saturated solution of ferrocene in DMF for 24 h. After 24 h, the crystals were removed from the dye solution and examined using optical microscopy.

Deinterpenetration of IRMOF-9 in the Presence of Reichardt's Dye

A stock solution of 1:1 DCM:DMF, Et₄NBr (0.16 M), and Reichardt's dye (10 mM) was prepared. Separately, seven 4 mL glass, Teflon-capped vials were charged with IRMOF-9 that had previously been rinsed with DMF (3×10 mL, with 30 minutes in between rinses). To each of these vials, stock solution (0.25 mL) was added within the span of two minutes. The samples were then placed in an orbital shaker oven set to 26 °C and 70 rpm. The samples were removed one by one at designated time points (2 h, 3 h, 4 h, 5 h, 1 day, and 2 days), washed in DCM, and analyzed using optical microscopy.

Synthesis of Cadmium Selenide Quantum Dots (CdSe QDs)

CdSe QD synthesis was based on the protocol given by Landry *et al.*² The cadmium precursor solution was prepared by dissolving cadmium acetate (53 mg, 0.23 mmol) with oleic acid (0.6 mL, 1.90 mmol) and octadecene (5.5 mL, 17.2 mmol) in a 25 mL round bottom flask. The solution was then stirred at 130 °C for 20 minutes. The selenium precursor solution was prepared by dissolving selenium powder (99 mg, 1.25 mmol) in trioctylphosphine (5.5 mL, 12.3 mmol) in a 22 mL glass vial. The solution was sonicated at room temperature until the selenium powder was fully dissolved (ca. 5 minutes). To prepare the reaction solution, octadecene (10 mL) was heated and stirred (aggressive stirring of > 400 rpm is recommended) at 165 °C for 20 minutes in a separate 25 mL round bottom flask. From the (now heated) cadmium precursor solution, 1 mL of solution was

withdrawn and quickly added to the reaction solution simultaneously with 1 mL of the selenium precursor solution. After incubation for 5.5-6.5 minutes, the solution was withdrawn *via* syringe and cooled to room temperature.

To wash the product, 1 mL aliquots of the CdSe QD-containing solution were extracted and washed with 2 mL of ethanol, mixed thoroughly with a vortex shaker, and then subject to centrifugation at 3000 rpm for 5 minutes. The supernatant was removed (the solution should appear oily at the bottom), and ethanol (2-3 mL) was added. The solution was again mixed with the vortex shaker and subject to centrifugation at 3000 rpm for 5 minutes. The samples were washed in this way until the CdSe QDs could be seen along the walls of the tube as a fine yellow precipitate and no longer appeared oily. The QDs were then resuspended and combined in fresh DCM (2 mL). QD size was determined by analysis with UV-vis absorption spectroscopy according to the method described by Jasieniak *et al.*³

Cadmium Selenide Quantum Dot Dye Exclusion

A previously prepared sample of deinterpenetrated IRMOF-9 (15 mg, suspended in DMF) was rinsed in DCM 3 times, with 20 minutes in between each rinse. The DCM was decanted, and 2 mL of CdSe QD solution (previously washed in DCM) was added. The deinterpenetrated IRMOF-9 crystals were immersed in the CdSe QD solution for 2 days and subsequently analyzed *via* optical microscopy under UV light and white light.

MOF Activation.

MOF samples were synthesized as described above and activated by one of two methods.

Method 1. After rinsing with DMF, they were subsequently rinsed in DCM (three rinses, 15 mL per rinse, waiting 30 minutes in between rinses) and subsequently transferred to long stemmed

sorption analysis tubes. The samples (~70-90 mg) were then activated at room temperature under reduced pressure (~200 mTorr) for 24-48 hours.

Method 2. Samples of deinterpenetrated IRMOF-9 in DMF were activated using flowing supercritical CO₂.⁴ After loading into a stainless steel sample tube, the MOF was subject to a 2 mL/min flow of liquid CO₂ at room temperature, then a 2 mL/min flow of supercritical CO₂ at 55 °C for 2 hours, and finally a 1 mL/min flow of supercritical CO₂ at 55 °C for 1 hour. Samples were otherwise treated as previously described.⁴

Gas Sorption Measurements and Data Analysis.

The activated samples were analyzed using N₂ sorption at 77 K using 99.999% purity N₂ (AIRGAS Inc.), and the sorption isotherms were obtained via a 3Flex Adsorption Analyzer (Micromeritics Instrument Corp.).

N₂ adsorption isotherms were fit using a proprietary DFT model for cylindrical pores and oxide surface (Flex software v. 6.02, Micromeritics Instrument Corp.). No smoothing nor regularization was applied to the pore size distributions. The particular DFT model used for these calculations was chosen as it exhibited the lowest standard deviation with respect to the experimental data among available models. The pore size of the majority pores increased after deinterpenetration independent of the model used, supporting the contention that conversion from an interpenetrated framework (IRMOF-9) to a deinterpenetrated form occurs.

Digestion of MOF samples for NMR Analysis

MOF (ca. 5 mg) was sonicated in a mixture of 750 μ L perdeuterated dimethylsulfoxide and 50 μ L trifluoroacetic acid for five minutes, after which the solution became transparent to the naked eye. The resulting solution was then transferred to NMR tubes *via* filtration through 0.2 μ m PTFE syringe filters.

Preparation of the Conversion Mother Liquor for NMR Analysis

IRMOF-9 was subject to the deinterpenetration solution for 2 days. The mother liquor from this process was then collected, and the DMF/DCM was removed under reduced pressure *via* rotary vacuum evaporation. The resulting residue was then further dried under reduced pressure (~50 mTorr) overnight. The collected and dried residue was then resuspended in perdeuterated dimethylsulfoxide (750 μ L) and transferred to an NMR tube after filtration through a 0.2 μ m PTFE syringe filter.

Modeling of Pore Diameters.

The pore aperture diameters and internal pore diameters of IRMOF-9 and IRMOF-10 were calculated using PoreBlazer v. 3.02^{5,6} using a probe diameter of 3.31 Å:

Pore Measurement	IRMOF-9	IRMOF-10
Pore Aperture Diameter (Å)	8.14	11.65
Internal Pore Diameter (Å)	11.01	20.78

Table S1: Pore diameters of IRMOF-9 and IRMOF-10 calculated from their respective crystallographic models.

Supplemental Figures

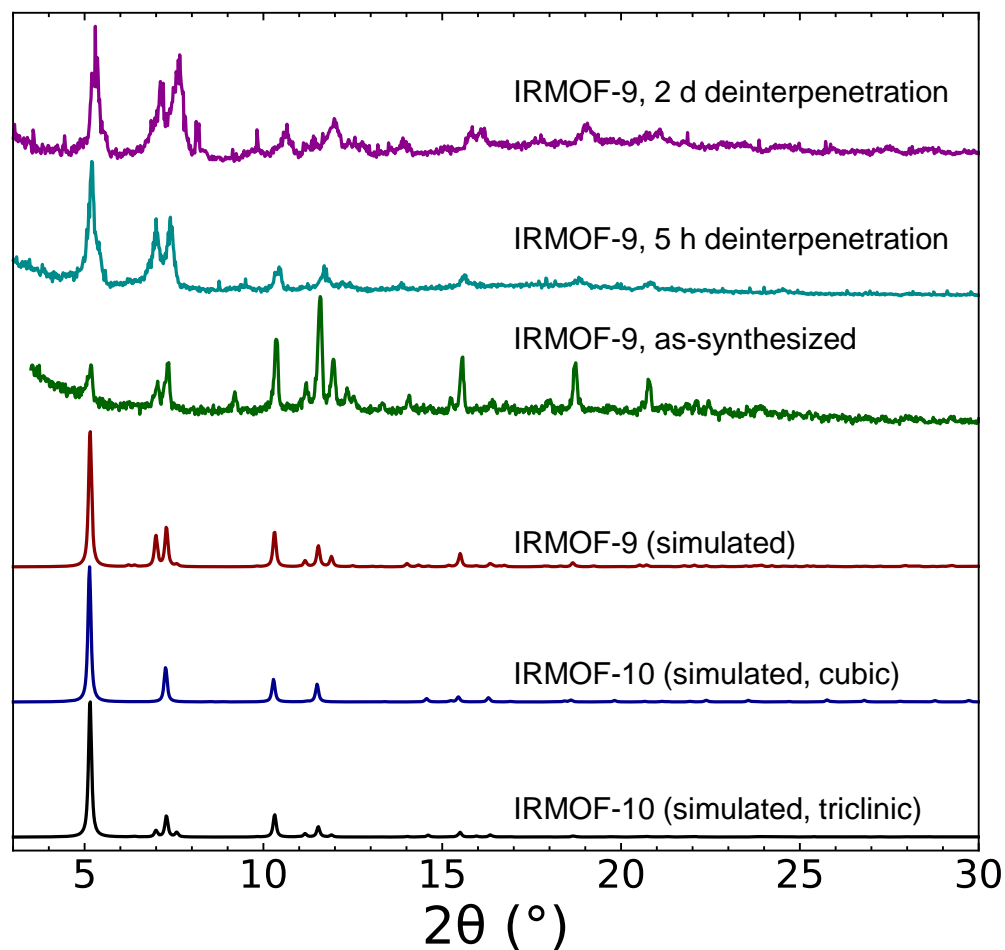


Figure S1. X-ray diffraction patterns of IRMOF-9 before and after exposure to deinterpenetration conditions for 5 h and 2 d. Simulated diffraction patterns for both IRMOF-9 and IRMOF-10 are provided. “Cubic” IRMOF-10 is that obtained by subtraction from the structure of IRMOF-12;⁷ “triclinic” IRMOF-10 is obtained by subtracting one interpenetrated partner in IRMOF-9.

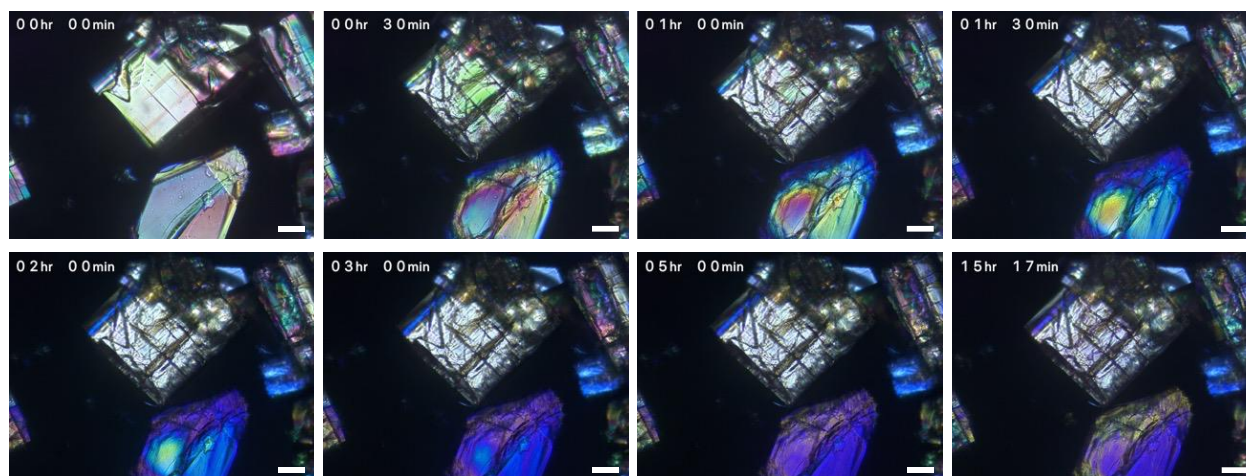


Figure S2. Timelapse images monitoring the deinterpenetration of IRMOF-9 *in situ* under crossed polarizers. As the reaction proceeds, crystal fracturing occurs (represented clearly in the center crystal). However, the crystal size does not change within the limit of detection of the imaging, consistent with selective dissolution. The color change observed in the bottom crystal is consistent with a phase change. Scale bar: 50 μm .

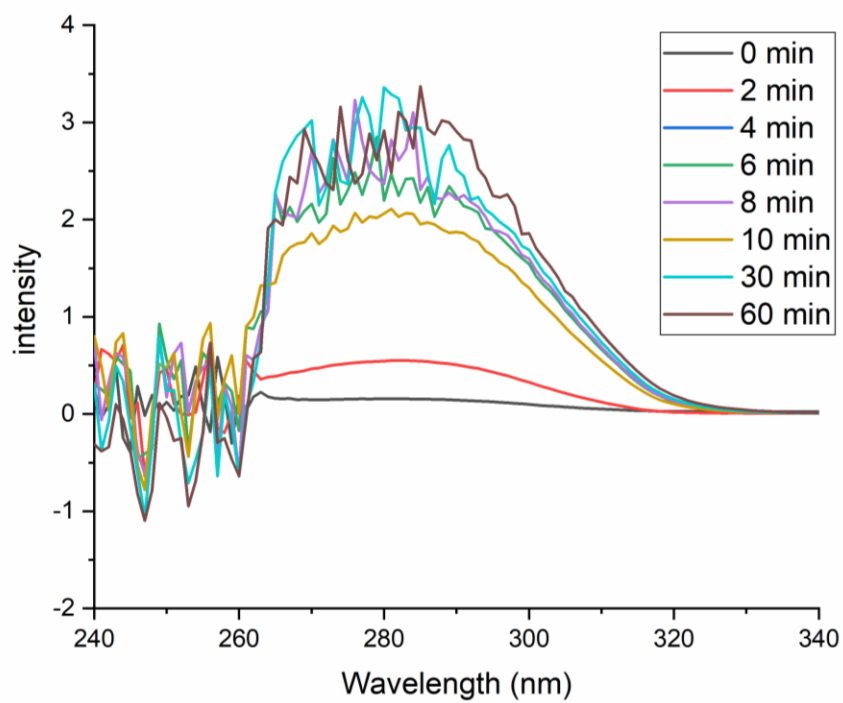


Figure S3. UV-vis absorbance spectra during the deinterpenetration process of IRMOF-9 *via* Et₄NBr solution. The peak centered at 285 nm corresponds to free 4,4'-biphenyldicarboxylic acid. Data were obtained at ambient temperature.

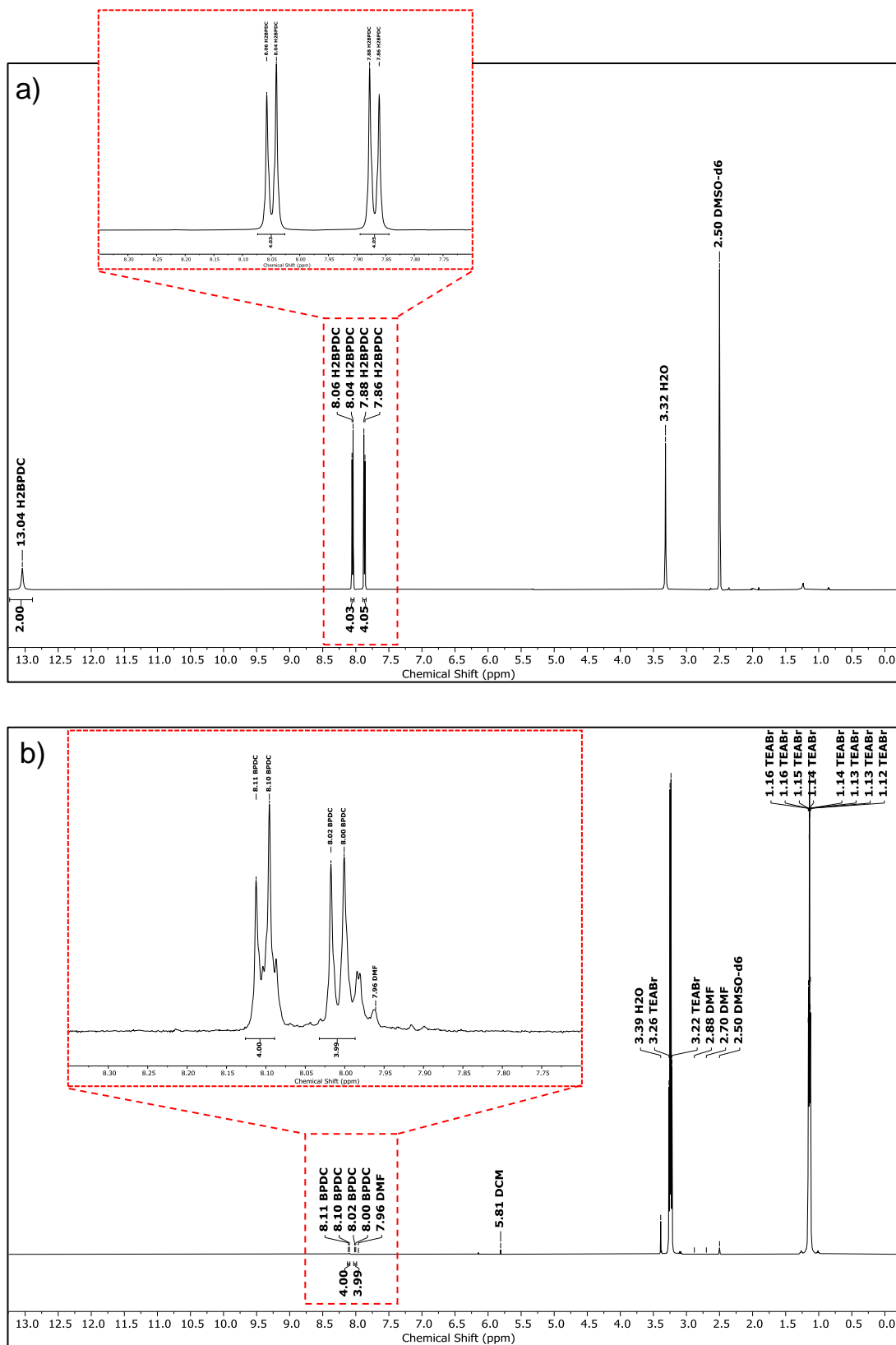


Figure S4. ^1H NMR of a) H_2BPDC in DMSO-d_6 and b) the mother liquor from the deinterpenetration of IRMOF-9 after 2 days in DMSO-d_6 .

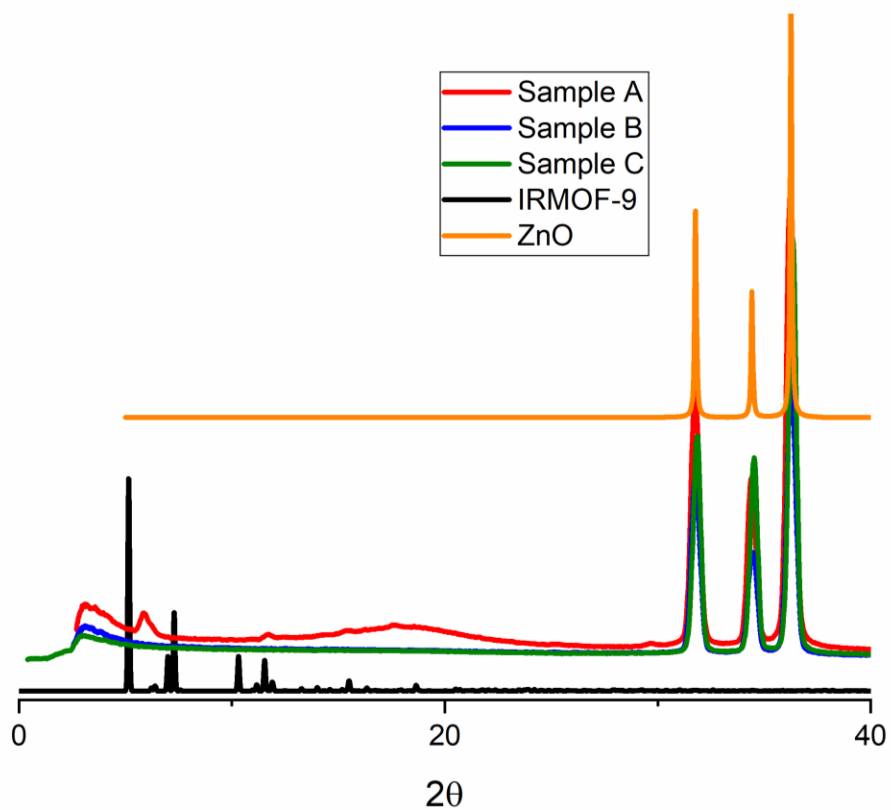


Figure S5. Powder X-ray diffraction patterns of samples from three different batches (blue, red, green) of powder obtained from mother liquor of the synthesis of deinterpenetrated IRMOF-9. Also shown is inorganic ZnO (orange) and IRMOF-9 prior to deinterpenetration (black).

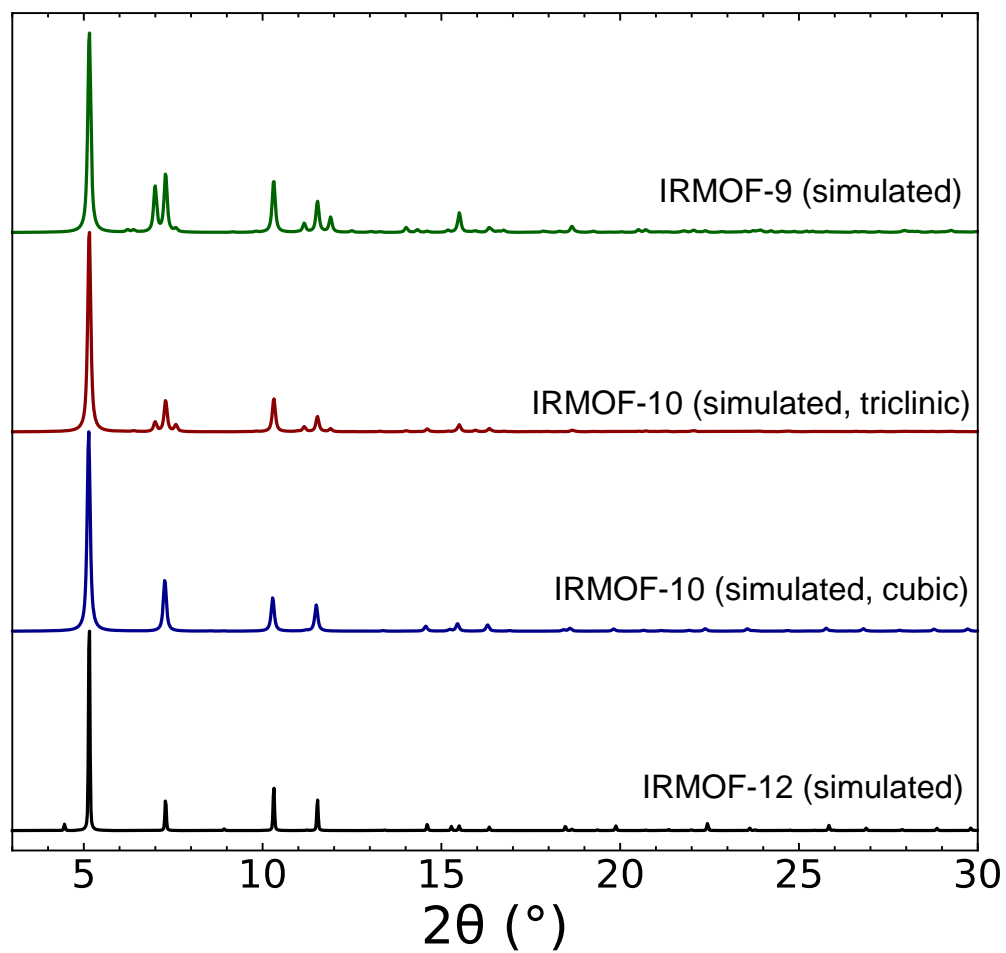


Figure S6. Calculated X-ray diffraction patterns for IRMOF-9, IRMOF-10 triclinic (red), IRMOF-10 cubic (blue), and IRMOF-12 (green).

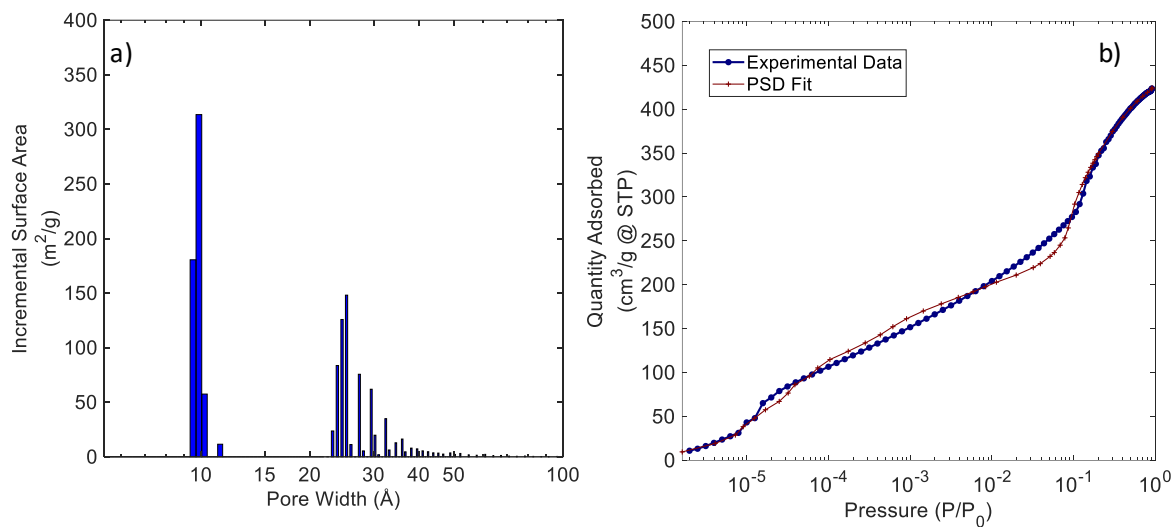


Figure S7. a) Pore diameter distribution for IRMOF-9 based on a DFT fit. The majority pore diameter is 9.9 Å. (Figure S7a is a reproduction of Figure 2c in the manuscript, reproduced here for convenience). b) Goodness of fit for IRMOF-9. The standard deviation of fit is 7.06 cm³/g @ STP.

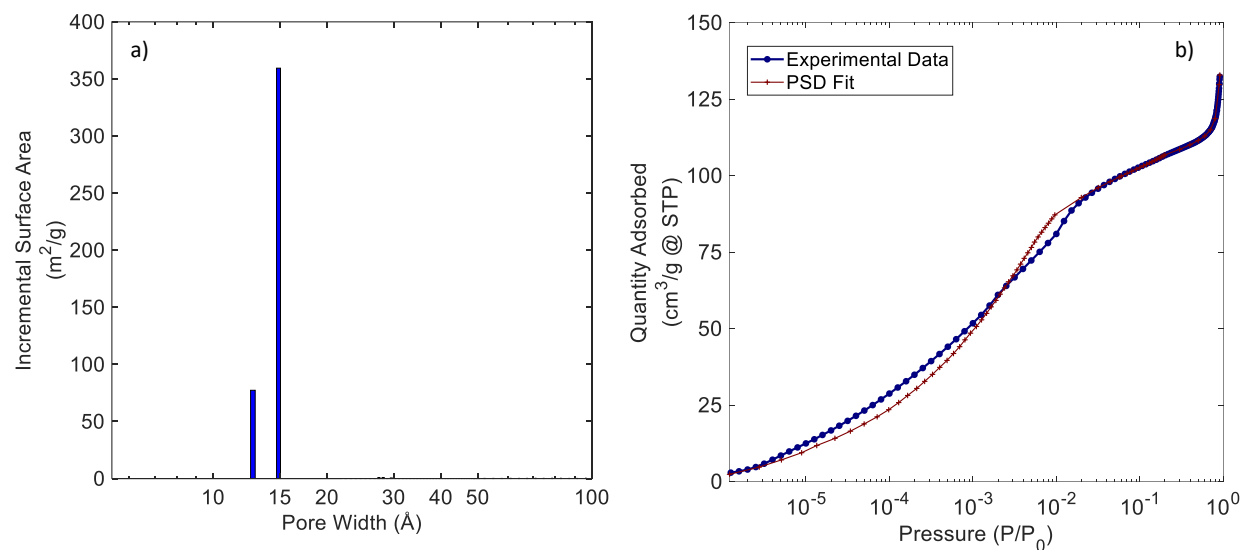


Figure S8. a) Pore diameter distribution for deinterpenetrated IRMOF-9 based on DFT fit. The majority pore diameter is 14.9 Å. (Figure S8a is a reproduction of Figure 2d in the manuscript, reproduced here for convenience). b) Goodness of fit for deinterpenetrated IRMOF-9. The standard deviation of fit is 2.14 cm³/g @ STP.

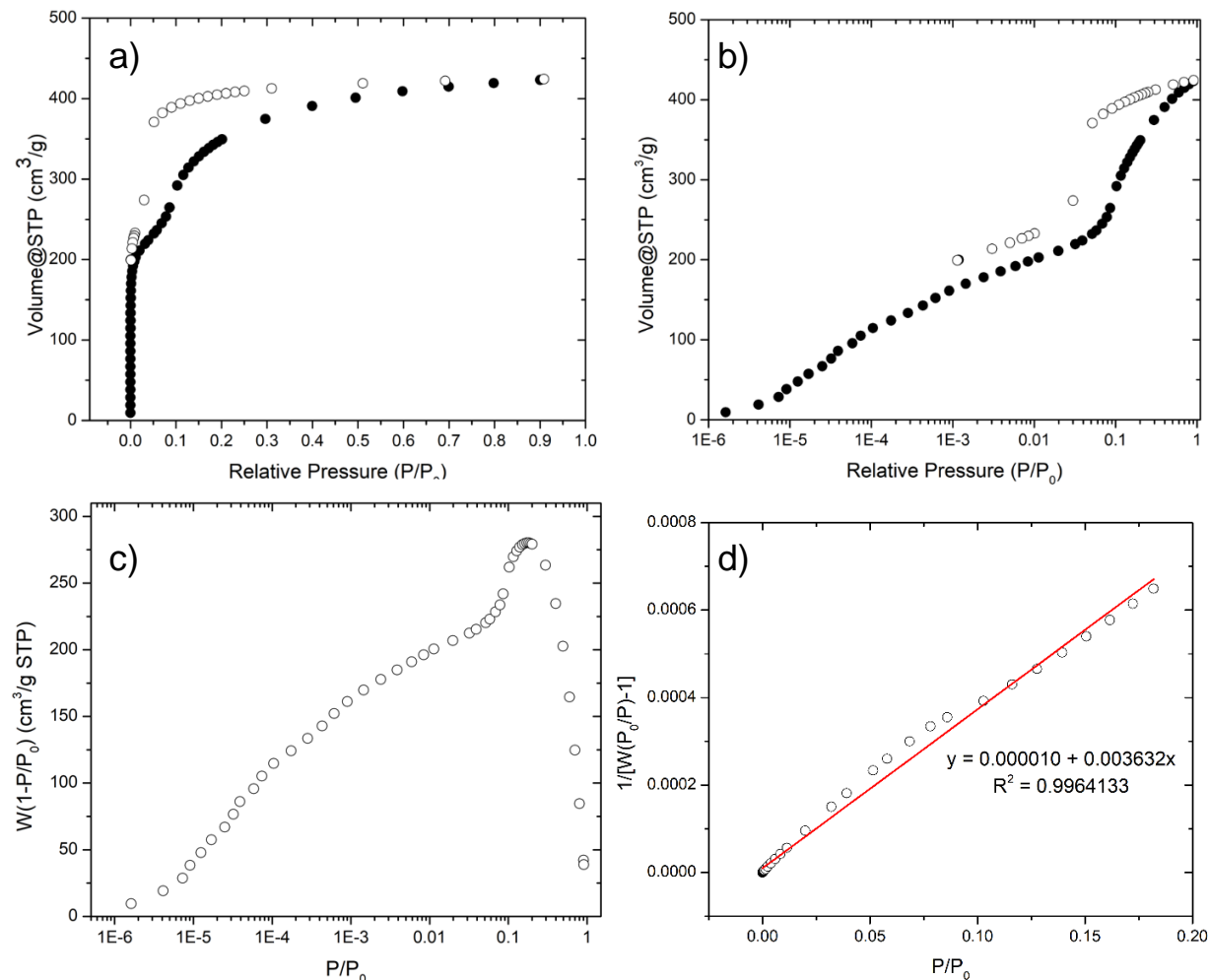


Figure S9. a) N₂ sorption isotherm of deinterpenetrated IRMOF-9 activated at room temperature and reduced pressure (~200 mTorr) for 48 hours. Figure S9a is a reproduction of Figure 2a in the main text, reproduced here for convenience (●, adsorption; ○, desorption). b) N₂ sorption isotherm in part (a) shown with a logarithmic scale (●, adsorption; ○, desorption). c) Consistency criterion plot for determining the P/P₀ range for the BET surface area analysis of plot (a). d) BET plot of IRMOF-9 using points below P/P₀ = 1.82×10⁻¹. The calculated BET surface area is 1195 m²/g. Non-linearity in the BET plot is attributed to the dynamic behavior of IRMOF-9 under sorption conditions; fits to strictly linear regions yield surface areas of 956 m²/g (P/P₀ range from 0 to 5.79×10⁻²) and 1315 m²/g (P/P₀ range from 1.03×10⁻¹ to 1.82×10⁻¹).

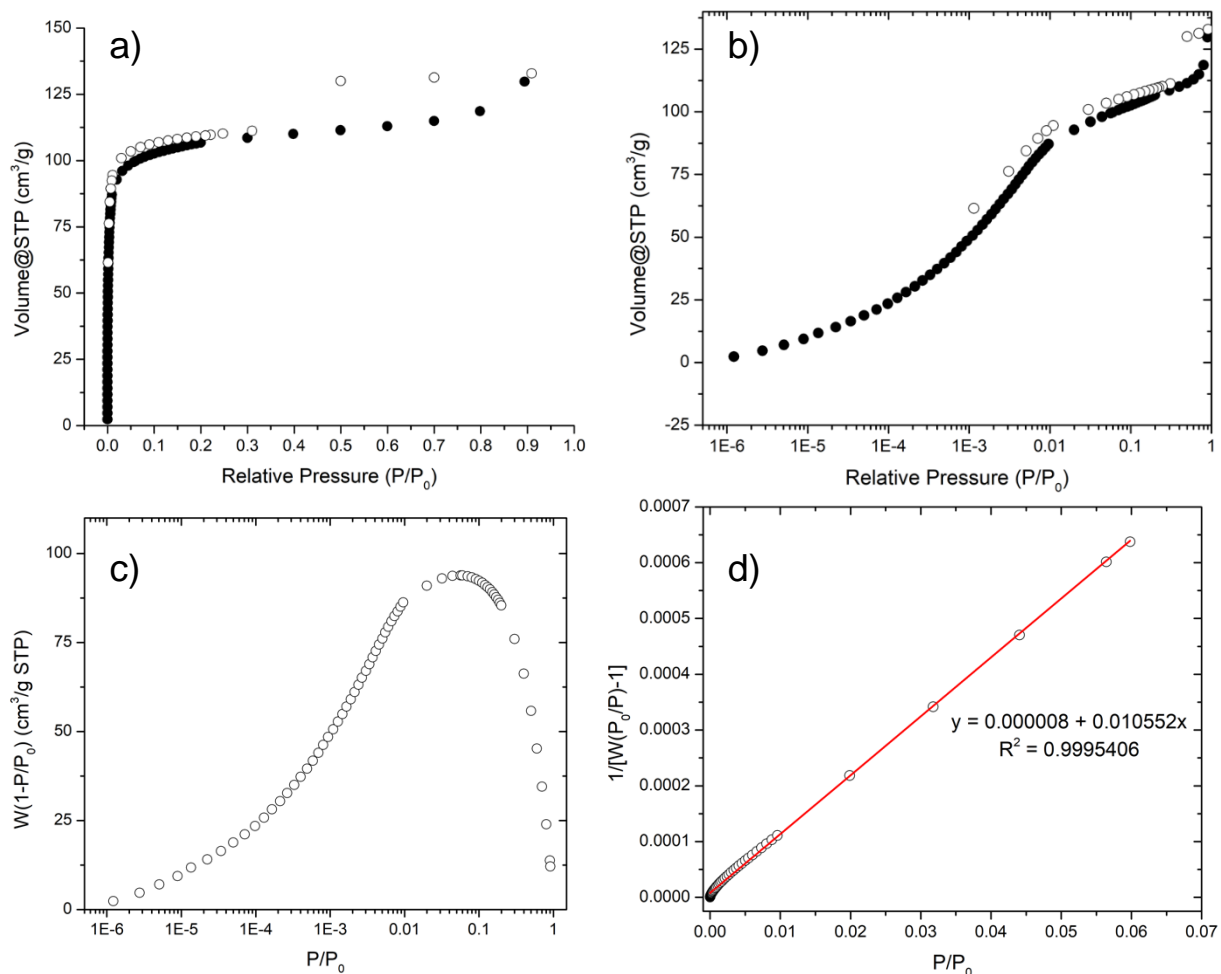


Figure S10. a) N₂ sorption isotherm of deinterpenetrated IRMOF-9 activated at room temperature and reduced pressure (~200 mTorr) for 24 hours. Figure S10a is a reproduction of Figure 2b in the main text, reproduced here for convenience (●, adsorption; ○, desorption). b) N₂ sorption isotherm in part (a) shown with a logarithmic scale (●, adsorption; ○, desorption). c) Consistency criterion plot for determining the P/P₀ range for the BET surface area analysis of plot (a). d) BET plot of deinterpenetrated IRMOF-9 using points below P/P₀ = 5.98 × 10⁻². The calculated BET surface area is 412 m²/g.

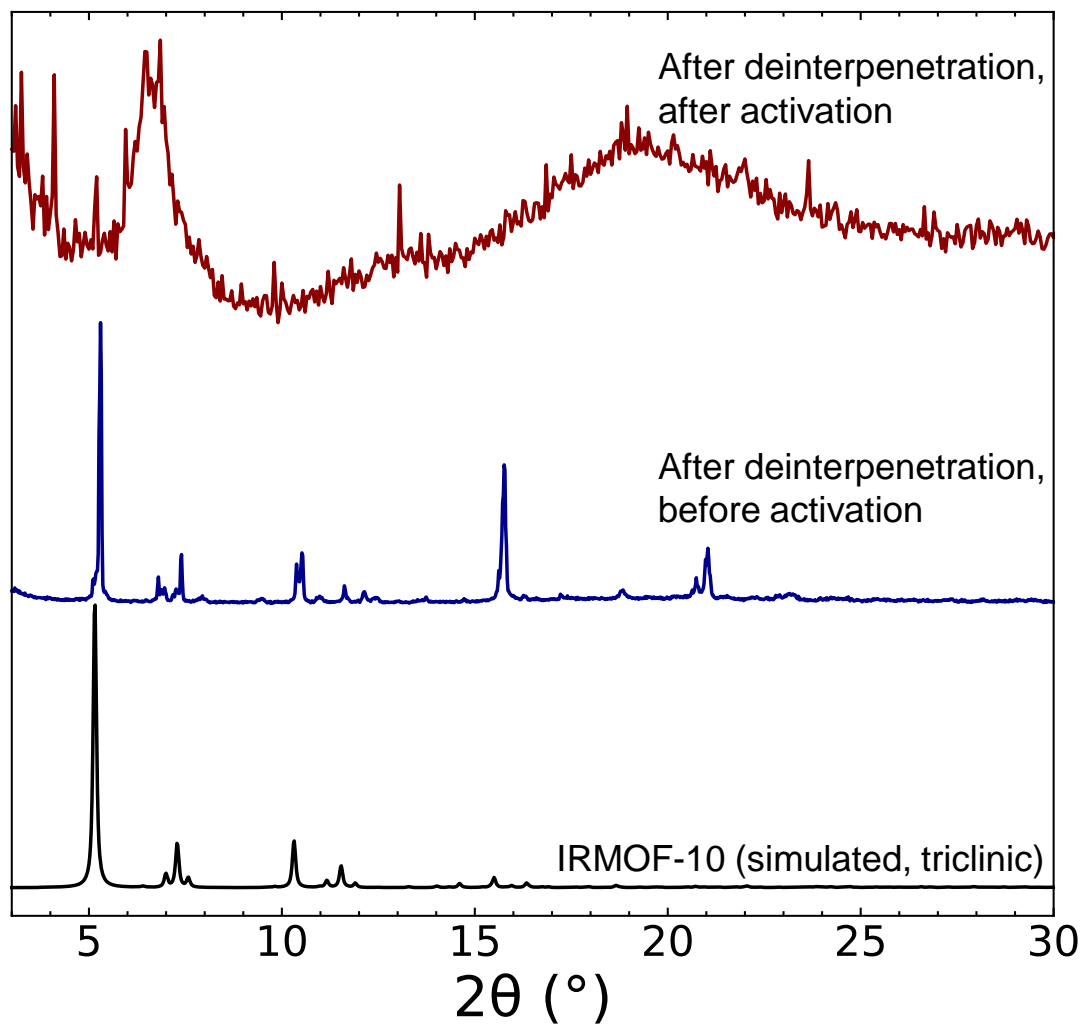


Figure S11. PXRD patterns of IRMOF-9 before and after activation from DCM under reduced pressure (~ 200 mTorr) at room temperature.

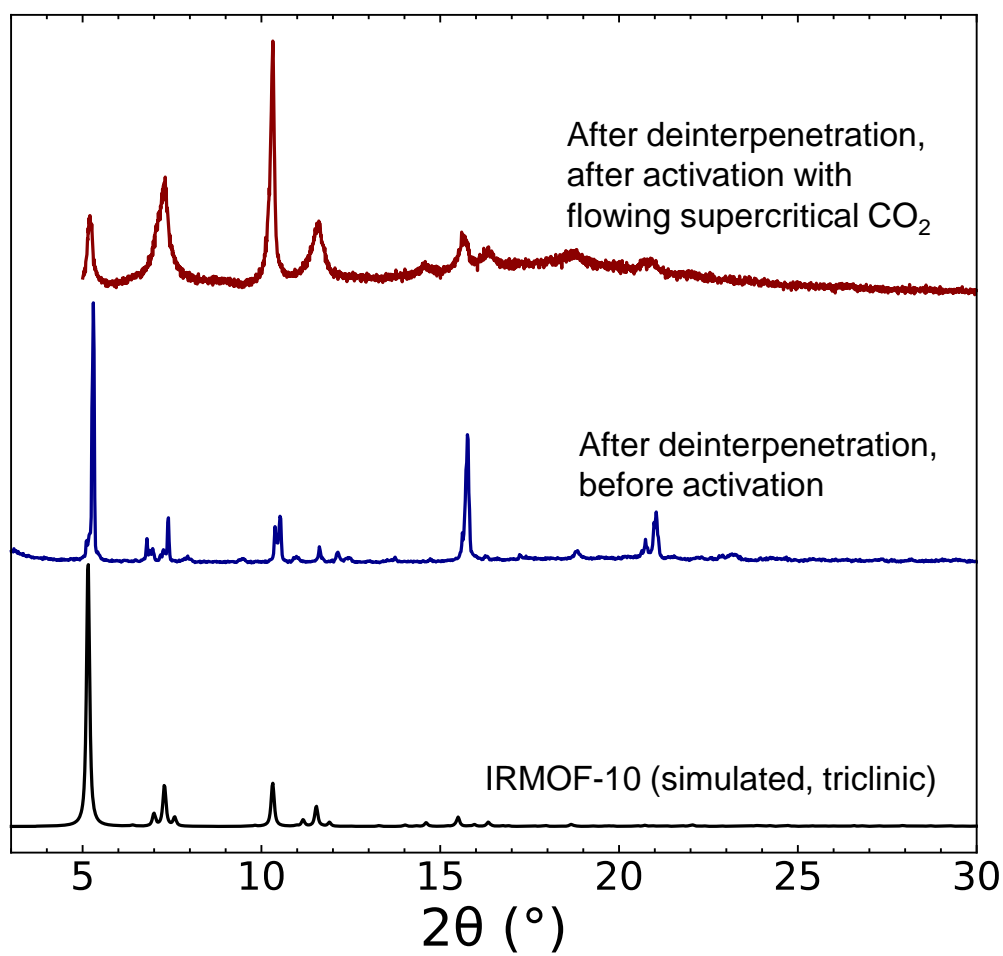


Figure S12. PXRD patterns of IRMOF-9 before and after activation flowing supercritical CO_2 .

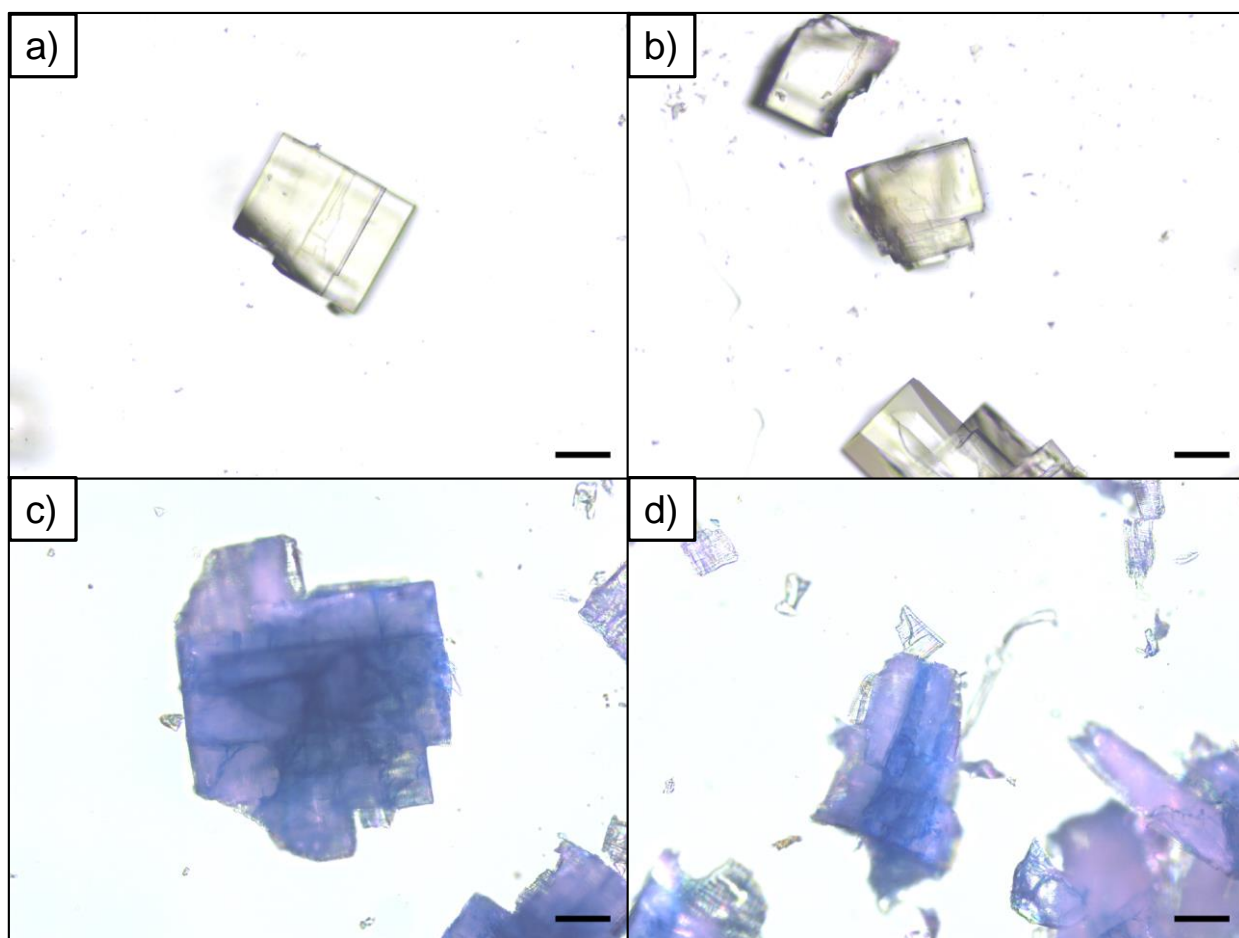


Figure S13. Optical microscope images of a) an IRMOF-9 crystal after Reichardt's dye size exclusion test in DMF (10 mM), b) the cross section of the IRMOF-9 crystal (after Reichardt's dye exclusion test in DMF, 10 mM), c) a deinterpenetrated IRMOF-9 crystal after *in situ* Reichardt's dye (10 mM) size exclusion test, washed in DMF prior to examination, and d) the cross section of the deinterpenetrated IRMOF-9 crystal (after *in situ* Reichardt's dye, 10 mM, size exclusion test, washed in DMF). All samples were immersed in mineral oil for imaging to prevent hydrolysis. Scale bar: 50 μm .

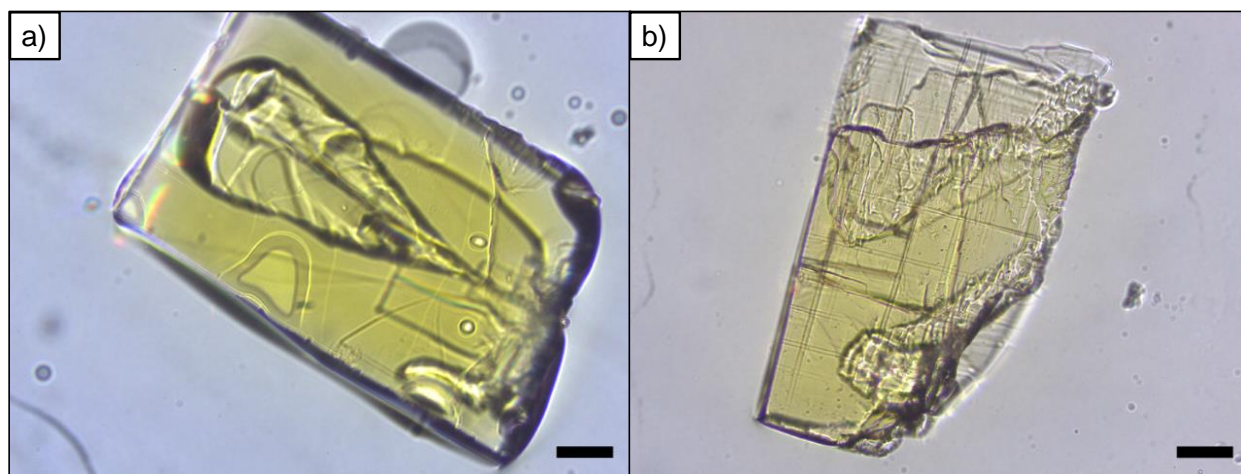


Figure S14. Ferrocene incorporation into a) IRMOF-9 and b) deinterpenetrated IRMOF-9 (right). Scale bar: 100 μm .

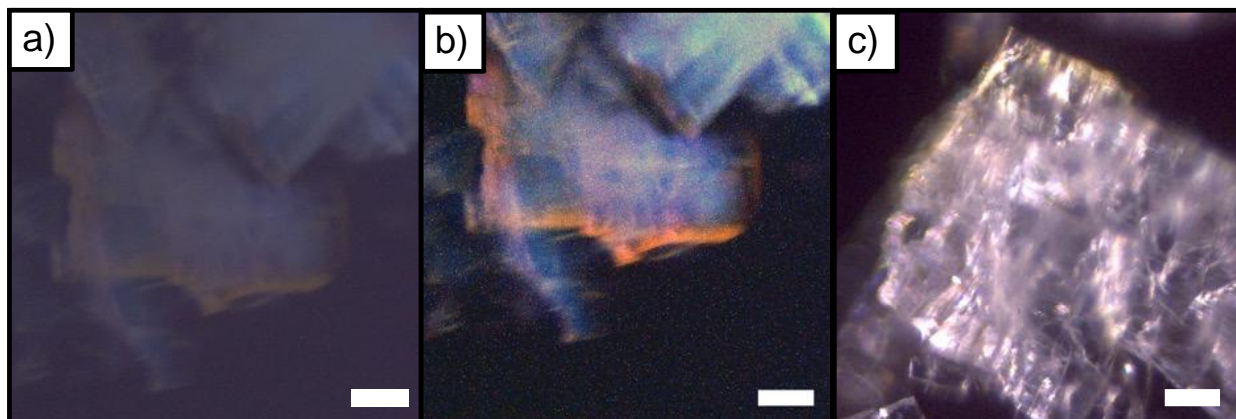


Figure S15. Optical microscope image of a) deinterpenetrated IRMOF-9 after being immersed in a dispersion of CdSe quantum dots (ca. 2 nm diameter) for 12 hours under UV light. b) Contrast-enhanced version of panel (a) showing regions where surface-adsorbed quantum dots fluoresce (red-orange color). c) Deinterpenetrated IRMOF-9 after being immersed in CdSe quantum dots (ca. 2 nm diameter) for 12 hours under white light. Scale bar: 100 μm .

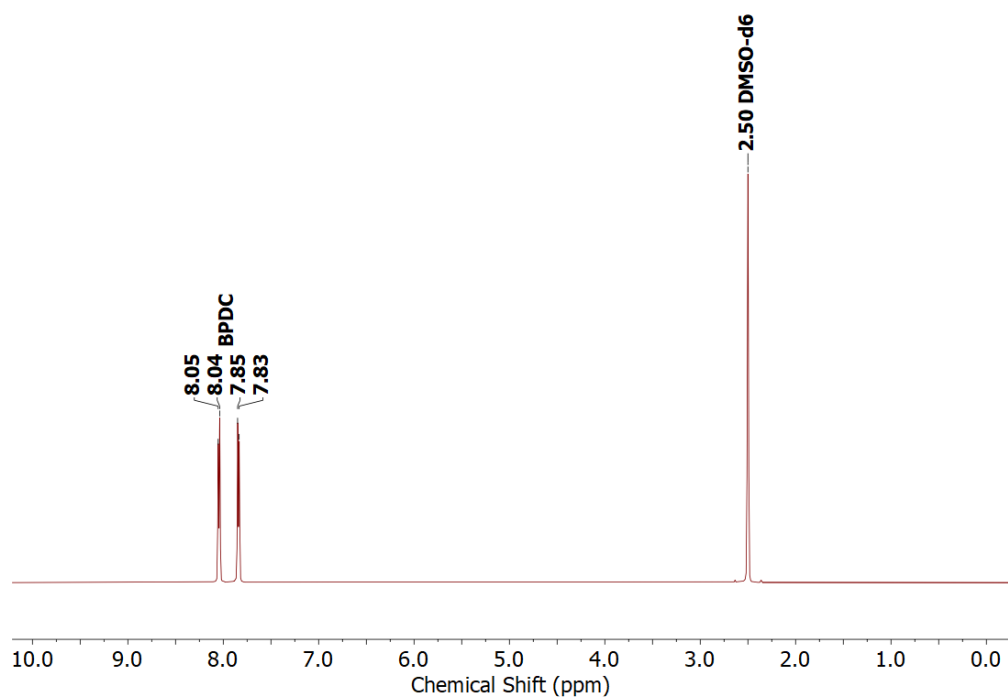


Figure S16: ^1H NMR of digested IRMOF-9 in DMSO-d₆.

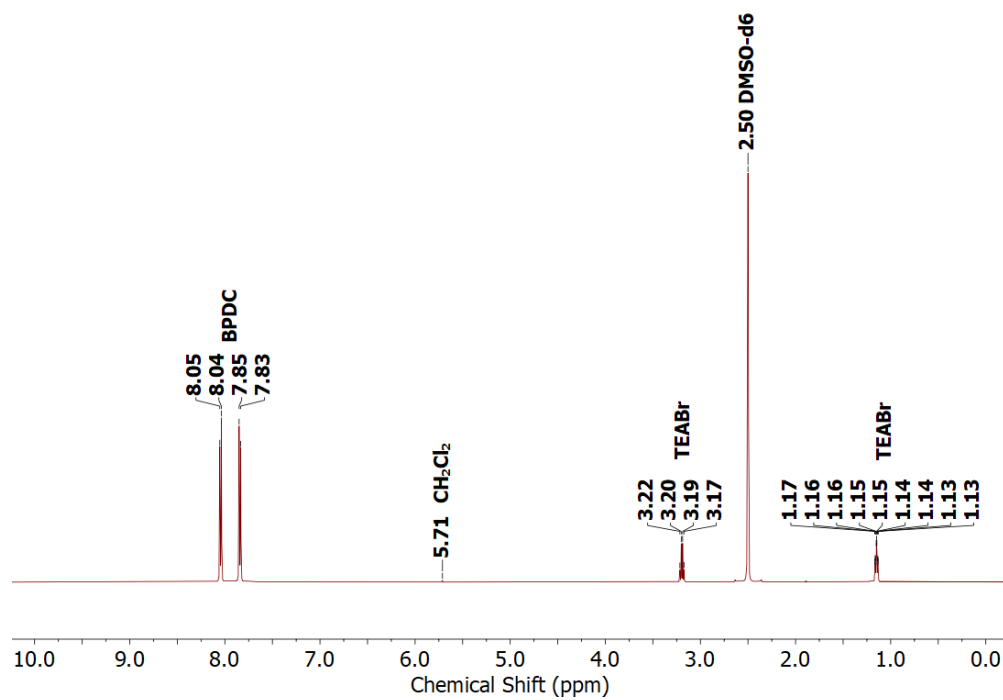


Figure S17: ^1H NMR of digested IRMOF-9 after deinterpenetration in DMSO-d_6 .

References

1. Rowsell, J. L. C.; Yaghi, O. M., Effects of Functionalization, Catenation, and Variation of the Metal Oxide and Organic Linking Units on the Low-Pressure Hydrogen Adsorption Properties of Metal–Organic Frameworks. *Journal of the American Chemical Society* **2006**, *128*, 1304-1315.
2. Landry, M. L.; Morrell, T. E.; Karagounis, T. K.; Hsia, C.-H.; Wang, C.-Y., Simple Syntheses of CdSe Quantum Dots. *J. Chem. Educ.* **2014**, *91*, 274-279.
3. Jasieniak, J.; Smith, L.; van Embden, J.; Mulvaney, P.; Califano, M., Re-examination of the Size-Dependent Absorption Properties of CdSe Quantum Dots. *J. Phys. Chem. C* **2009**, *113*, 19468-19474.
4. Liu, B.; Wong-Foy, A. G.; Matzger, A. J., Rapid and Enhanced Activation of Microporous Coordination Polymers by Flowing Supercritical CO₂. *Chem. Commun.* **2013**, *49*, 1419-1421.
5. Sarkisov, L.; Harrison, A., Computational Structure Characterisation Tools in Application to Ordered and Disordered Porous Materials. *Molecular Simulation* **2011**, *37*, 1248-1257.
6. Sarkisov, L.; Bueno-Perez, R.; Sutharson, M.; Fairen-Jimenez, D., Materials Informatics with PoreBlazer v4.0 and the CSD MOF Database. *Chem. Mater.* **2020**, *32*, 9849-9867.
7. Eddaoudi, M.; Kim, J.; Rosi, N.; Vodak, D.; Wachter, J.; O'Keeffe, M.; Yaghi, O. M., Systematic Design of Pore Size and Functionality in Isoreticular MOFs and their Application in Methane Storage. *Science* **2002**, *295*, 469-472.